Binary Signaling of Correlated Sources Over Orthogonal Multiple-Access Channels

Tyson P. Mitchell, Fady Alajaji, and Tamás Linder

***Abstract*—The optimal energy allocations for minimizing the joint symbol error rate for binary signaling of two correlated sources over the orthogonal multiple-access Gaussian channel under joint maximum *a priori* (MAP) detection are determined. An exact expression for the system's probability of joint symbol error, as well as its union bound, is derived. Analytic minimization of the union bound reveals that the optimal energy allocation coincides with that of nonuniform binary signaling over the single-user additive white Gaussian noise channel. It is also shown numerically that the optimal energies that minimize the union bound also minimize the exact probability of error. Finally, it is shown via simulations for strongly biased sources that the use of joint MAP detection over two independent single-user systems leads to significant gains.**

***Index Terms*—Error analysis, joint source–channel coding, MAP detection, multiple-access channels, nonuniform sources.**

I. Introduction

We consider the joint source–channel coding problem of designing an optimal source-matched modulation scheme for the reliable transmission of binary correlated sources over the orthogonal multiple access Gaussian channel (OMAGC) without the explicit use of data compression or error-correcting codes. The construction of such low-delay, low-complexity signaling schemes has pertinent applications to wireless sensor networks where multiple sensors observe correlated data and relay them in real-time to the base station [1]. In such wireless systems, delay, power, complexity, and scalability constraints often restrict the use of powerful coding and signal processing methods, and thus each sensor often performs a simple signaling function when sending the data it senses.

In a related prior work, considering orthogonal and nonorthogonal signaling separately, Korn *et al.* [2] derive optimal energy allocations for uncoded single-user binary communications over a point-to-point AWGN channel with non-equal symbol probabilities. In a follow-up work, Ipatov [3] re-derives the results of [2] for coherent detection using a simplified treatment. Motivated by applications to sensor networks and the fact that nonuniform sources are good models for many types of data (e.g., see [4]), in this letter we extend the coherent detection results from [2], to the two-user OMAGC and a 2-D nonuniform correlated source. In other related works, various signal set designs for systems with non-equal symbol probabilities were studied in [5]–[9] (to name a few); see also [10]–[12] for works on the error analysis of such systems.

Manuscript received April 24, 2015; revised May 26, 2015; accepted June 9, 2015. Date of publication June 18, 2015; date of current version October 9, 2015. This work was supported in part by NSERC of Canada. The associate editor coordinating the review of this paper and approving it for publication was M. Xiao.

The authors are with the Department of Mathematics and Statistics, Queen's University, Kingston, ON K7L 3N6, Canada (e-mail: tyson.mitchell@queensu.ca; fady@mast.queensu.ca; linder@mast.queensu.ca).

Digital Object Identifier 10.1109/LWC.2015.2446986

The contributions of this work are organized as follows. In Section II, the system set-up is presented. In Section III, an exact expression for the system's joint symbol error rate under joint MAP decoding and the union upper bound on the symbol error rate are established. Making use of its simplified form, the union bound is analytically minimized over the set of signaling energies. It is then shown numerically that the signaling energies that optimize the union bound also minimize the exact symbol error rate and are hence optimal. Performance results illustrating the benefits of using the optimal energy signaling schemes under joint MAP detection are presented in Section IV. Section V concludes the letter.

II. System Model

The system consists of Transmitters 1 and 2, two independent AWGN channels, and a joint MAP detector. Transmitter i (with $i = 1, 2$) can be described as follows: let

$$s_{i0}(t) = \sqrt{E_{i0}}\psi_1^{(i)}(t) \text{ and } s_{i1}(t) = \sqrt{E_{i1}}\psi_2^{(i)}(t)$$

be arbitrary binary transmission signals with energies E_{i0} and E_{i1}, respectively, such that s_{i0} has probability p_i with $0 \le p_i \le 0.5$ and s_{i1} has probability $1 - p_i$, for $i = 1, 2$, and where $\psi_j^{(i)} : [0, T] \mapsto \mathbb{R}$ has unit energy for $i, j = 1, 2$. Further, $\psi_1^{(i)}$ and $\psi_2^{(i)}$ have correlation

$$\gamma_i = \int_0^T \psi_1^{(i)}(t)\psi_2^{(i)}(t)dt.$$

Thus, Transmitter i will have an average energy per symbol of

$$E_i = E_{i0}p_i + E_{i1}(1 - p_i), \tag{1}$$

$i = 1, 2$. At each transmission instance, Transmitters 1 and 2 send $S_1 \in \mathcal{S}_1 = \{s_{10}, s_{11}\}$ and $S_2 \in \mathcal{S}_2 = \{s_{20}, s_{21}\}$, respectively, over the independent AWGN channels, where the random source pair (S_1, S_2) has joint probability mass function given by

$$\begin{aligned} p_{S_1,S_2}(s_{10}, s_{20}) &= 1 - (1 - p_1) - (1 - p_2) + p_{11} \\ p_{S_1,S_2}(s_{10}, s_{21}) &= (1 - p_1) - p_{11} \\ p_{S_1,S_2}(s_{11}, s_{20}) &= (1 - p_2) - p_{11} \\ p_{S_1,S_2}(s_{11}, s_{21}) &= p_{11}. \end{aligned}$$

Note that p_{11} can be expressed as

$$p_{11} = \rho\sqrt{p_1(1 - p_1)p_2(1 - p_2)} + (1 - p_1)(1 - p_2)$$

where ρ is the correlation coefficient of the underlying jointly distributed binary source pair $(U_1, U_2) \in \{0, 1\}^2$ defined by letting $U_i = 0$ if $S_i = s_{i0}$ and $U_i = 1$ if $S_i = s_{i1}$ for $i = 1, 2$.

The received information at the output of the matched filter is given by the random pair (R_1, R_2) such that $R_i = s_i + N_i$, where $s_i \in \mathcal{S}_i$ and N_i is zero-mean Gaussian noise with variance σ_i^2, for $i = 1, 2$, such that N_1 and N_2 are independent. The joint MAP detector, which is optimal in terms of minimizing

the probability of joint symbol error, receives (r_1, r_2)—the realizations of (R_1, R_2)—and implements the following MAP decision rule

$$\begin{aligned}\hat{\boldsymbol{s}} &= \underset{(s_1,s_2)\in\mathcal{S}_1\times\mathcal{S}_2}{\arg\max}\ P(S_1 = s_1, S_2 = s_2 | R_1 = r_1, R_2 = r_2)\\ &= \underset{\boldsymbol{s}\in\mathcal{S}_1\times\mathcal{S}_2}{\arg\max}\ h(\boldsymbol{s})\end{aligned}$$

where $\boldsymbol{s} = (s_1, s_2)$ and

$$h(\boldsymbol{s}) = \ln p_{S_1,S_2}(s_1, s_2) - \frac{s_1^2 - 2r_1 s_1}{2\sigma_1^2} - \frac{s_2^2 - 2r_2 s_2}{2\sigma_2^2} \quad (2)$$

so that $\hat{\boldsymbol{s}} = (\hat{s}_1, \hat{s}_2) \in \mathcal{S}_1 \times \mathcal{S}_2$ is the MAP estimate of the transmitted pair. Note that $s_1^2 = E_{1i}$ and $s_2^2 = E_{2j}$ are the energies of the respective signals, where $i, j \in \{0, 1\}$.

III. Probability of Symbol Error Analysis

A. Probability of Symbol Error

A symbol error event, e, occurs when $\boldsymbol{s} \neq \hat{\boldsymbol{s}}$, where $\boldsymbol{s}$ and $\hat{\boldsymbol{s}}$ are defined above. Setting $\boldsymbol{s}_{00} = (s_{10}, s_{20})$, $\boldsymbol{s}_{01} = (s_{10}, s_{21})$, $\boldsymbol{s}_{10} = (s_{11}, s_{20})$, and $\boldsymbol{s}_{11} = (s_{11}, s_{21})$, the probability of error, $P(e)$, can be expressed as

$$\begin{aligned}P(e) &= \sum_{\boldsymbol{k}\in\{0,1\}^2} P(\hat{\boldsymbol{s}} \neq \boldsymbol{s}_{\boldsymbol{k}} | \boldsymbol{k}) P(\boldsymbol{s}_{\boldsymbol{k}})\\ &= 1 - \sum_{\boldsymbol{k}\in\{0,1\}^2} P(\hat{\boldsymbol{s}} = \boldsymbol{s}_{\boldsymbol{k}} | \boldsymbol{k}) P(\boldsymbol{s}_{\boldsymbol{k}}) \quad (3)\end{aligned}$$

where $P(\hat{\boldsymbol{s}} = \boldsymbol{s}_{\boldsymbol{k}} | \boldsymbol{k})$ is the probability of correct detection given that $\boldsymbol{s}_{\boldsymbol{k}} \triangleq (s_{1k_1}, s_{2k_2})$, where $\boldsymbol{k} \triangleq (k_1, k_2) \in \{0, 1\}^2$, was transmitted, and $P(\boldsymbol{s}_{\boldsymbol{k}})$ is the probability that $\boldsymbol{s}_{\boldsymbol{k}}$ was transmitted. Let

$$\tilde{h}(\boldsymbol{s}) = \ln p_{S_1,S_2}(s_1, s_2) - \frac{s_1^2 - 2R_1 s_1}{2\sigma_1^2} - \frac{s_2^2 - 2R_2 s_2}{2\sigma_2^2}$$

be our MAP detection metric based on (2). Then, we can write

$$\begin{aligned}P(\hat{\boldsymbol{s}} = \boldsymbol{s}_{\boldsymbol{k}} | \boldsymbol{k}) &= P\left(\tilde{h}(\boldsymbol{s}_{\boldsymbol{k}}) = \max_{\boldsymbol{j}\in\{0,1\}^2} \tilde{h}(\boldsymbol{s}_{\boldsymbol{j}}) \middle| \boldsymbol{k}\right)\\ &= P\left(\bigcap_{\boldsymbol{j}\neq\boldsymbol{k}} \left\{\tilde{h}(\boldsymbol{s}_{\boldsymbol{k}}) > \tilde{h}(\boldsymbol{s}_{\boldsymbol{j}})\right\} \middle| \boldsymbol{k}\right)\\ &= P\left(\bigcap_{\boldsymbol{j}\neq\boldsymbol{k}} \left\{V_{\boldsymbol{j}}^{(\boldsymbol{k})} < 0\right\} \middle| \boldsymbol{k}\right) \quad (4)\end{aligned}$$

where $V_{\boldsymbol{j}}^{(\boldsymbol{k})} = \tilde{h}(\boldsymbol{s}_{\boldsymbol{j}}) - \tilde{h}(\boldsymbol{s}_{\boldsymbol{k}})$ for $\boldsymbol{j}, \boldsymbol{k} \in \{0, 1\}^2$. Each $V_{\boldsymbol{j}}^{(\boldsymbol{k})}$ is a random variable. Moreover, since for $i = 1, 2$, R_i is Gaussian given $\boldsymbol{k}$, each $V_{\boldsymbol{j}}^{(\boldsymbol{k})}$ is Gaussian given $\boldsymbol{k}$. Further, since N_1 and N_2 are independent, R_1 and R_2 are independent, given $\boldsymbol{k}$. Now define $\boldsymbol{k}' \in \{0, 1\}$ such that $\boldsymbol{k}' = \boldsymbol{k} \oplus (1, 1)$, where $\oplus$ denotes component-wise modulo 2 addition. Then, we have

$$V_{\boldsymbol{k}'}^{(\boldsymbol{k})} = \alpha_{\boldsymbol{k}} + \sum_{\boldsymbol{j}\neq\boldsymbol{k},\boldsymbol{k}'} V_{\boldsymbol{j}}^{(\boldsymbol{k})} \quad (5)$$

where

$$\alpha_{\boldsymbol{k}} = \begin{cases} \ln \frac{P(s_{00})P(s_{11})}{P(s_{10})P(s_{01})} & \text{if } \boldsymbol{k} = (0,0), (1,1)\\ \ln \frac{P(s_{10})P(s_{01})}{P(s_{11})P(s_{00})} & \text{if } \boldsymbol{k} = (0,1), (1,0).\end{cases}$$

Thus, using (5), we can write (4) as

$$P\left(\left\{V_{\boldsymbol{k}'}^{(\boldsymbol{k})} < 0\right\} \bigcap \cap_{\boldsymbol{j}\neq\boldsymbol{k},\boldsymbol{k}'} \left\{V_{\boldsymbol{j}}^{(\boldsymbol{k})} < 0\right\} \middle| \boldsymbol{k}\right). \quad (6)$$

For example if $\boldsymbol{k} = (0, 0)$, then (6) is given by

$$P\left(V_{10}^{(00)} < 0, V_{01}^{(00)} < 0, V_{10}^{(00)} + V_{01}^{(00)} + \alpha_{00} < 0 \middle| \boldsymbol{k} = (0,0)\right).$$

By independence of N_1 and N_2, for $\boldsymbol{j} \neq \boldsymbol{k}, \boldsymbol{k}'$ we have

$$\begin{aligned}\mu_{\boldsymbol{j}}^{(\boldsymbol{k})} &\triangleq E\left[V_{\boldsymbol{j}}^{(\boldsymbol{k})} \middle| \boldsymbol{k}\right]\\ &= \ln \frac{P(s_{\boldsymbol{j}})}{P(s_{\boldsymbol{k}})} + \frac{s_{1k_1}^2 - s_{1j_1}^2}{2\sigma_1^2} + \frac{s_{2k_2}^2 - s_{2j_2}^2}{2\sigma_2^2}\\ &\quad + \frac{s_{1j_1} - s_{1k_1}}{\sigma_1^2} s_{1k_1} + \frac{s_{2j_2} - s_{2k_2}}{\sigma_2^2} s^{2k_2}\end{aligned}$$

and

$$\left(\sigma_{\boldsymbol{j}}^{(\boldsymbol{k})}\right)^2 \triangleq \mathrm{Var}\left(V_{\boldsymbol{j}}^{(\boldsymbol{k})} \middle| \boldsymbol{k}\right) = \frac{(s_{1k_1} - s_{1j_1})^2}{\sigma_1^2} + \frac{(s_{2k_2} - s_{2j_2})^2}{\sigma_2^2}.$$

It can be shown that (6) can be calculated as

$$\prod_{\boldsymbol{j}\neq\boldsymbol{k},\boldsymbol{k}'} Q\left(\frac{\mu_{\boldsymbol{j}}^{(\boldsymbol{k})}}{\sigma_{\boldsymbol{j}}^{(\boldsymbol{k})}}\right) - \Delta_{\boldsymbol{k}}$$

where

$$Q(x) \triangleq \frac{1}{2\pi} \int_x^\infty e^{-\frac{t^2}{2}} dt$$

is the Gaussian Q-function and $\Delta_{\boldsymbol{k}}$ given by

$$\Delta_{\boldsymbol{k}} = \int_{-\alpha_{\boldsymbol{k}}}^0 \int_{-v_1-\alpha_{\boldsymbol{k}}}^0 f_{V_{\boldsymbol{k}}}(v_1, v_2) dv_1 dv_2$$

if $\alpha_{\boldsymbol{k}} > 0$ and zero otherwise, where

$$f_{V_{\boldsymbol{k}}}(v_1, v_2) = \frac{1}{2\pi \prod_{\boldsymbol{j}\neq\boldsymbol{k},\boldsymbol{k}'} \sigma_{\boldsymbol{j}}^{(\boldsymbol{k})}} \exp\left\{-\frac{1}{2} \sum_{\boldsymbol{j}\neq\boldsymbol{k},\boldsymbol{k}'} \frac{\left(v_i - \mu_{\boldsymbol{j}}^{(\boldsymbol{k})}\right)^2}{\left(\sigma_{\boldsymbol{j}}^{(\boldsymbol{k})}\right)^2}\right\}.$$

where

$$i = \begin{cases} 1 \text{ if } \boldsymbol{j} \oplus \boldsymbol{k} = (1, 0)\\ 2 \text{ if } \boldsymbol{j} \oplus \boldsymbol{k} = (0, 1).\end{cases} \quad (7)$$

Thus, we have

$$P(e) = 1 - \sum_{\boldsymbol{k}\in\{0,1\}^2} \left[\prod_{\boldsymbol{j}\neq\boldsymbol{k},\boldsymbol{k}'} Q\left(\frac{\mu_{\boldsymbol{j}}^{(\boldsymbol{k})}}{\sigma_{\boldsymbol{j}}^{(\boldsymbol{k})}}\right) - \Delta_{\boldsymbol{k}}\right] P(\boldsymbol{s}_{\boldsymbol{k}}). \quad (8)$$

B. Analytic Optimization of the Union Bound

From (3) the union bound on $P(e)$, which we denote by $P_{UB}(e)$, is given by

$$P(e) \leq P_{UB}(e) \triangleq \sum_{\boldsymbol{k}\in\{0,1\}^2} P(\boldsymbol{s}_{\boldsymbol{k}}) \sum_{\boldsymbol{j}\neq\boldsymbol{k}} P(e_{\boldsymbol{j}\boldsymbol{k}})$$

where $e_{\boldsymbol{j}\boldsymbol{k}}$ is the event that $s_{\boldsymbol{j}}$ has a higher MAP metric then $s_{\boldsymbol{k}}$, and $P(e_{\boldsymbol{j}\boldsymbol{k}}) = P\left(\tilde{h}(\boldsymbol{s}_{\boldsymbol{j}}) > \tilde{h}(\boldsymbol{s}_{\boldsymbol{k}})\right) = 1 - P(V_{\boldsymbol{j}}^{(\boldsymbol{k})} < 0)$. Further,

$$1 - P\left(V_{\boldsymbol{j}}^{(\boldsymbol{k})} < 0\right) = 1 - Q\left(\frac{\mu_{\boldsymbol{j}}^{(\boldsymbol{k})}}{\sigma_{\boldsymbol{j}}^{(\boldsymbol{k})}}\right).$$

Thus, the union bound on the probability of symbol error becomes

$$P_{UB}(e) = \sum_{\boldsymbol{k}\in\{0,1\}^2} P(\boldsymbol{s_k}) \left[\sum_{\boldsymbol{j}\neq\boldsymbol{k}} 1 - Q\left(\frac{\mu_{\boldsymbol{j}}^{(\boldsymbol{k})}}{\sigma_{\boldsymbol{j}}^{(\boldsymbol{k})}}\right)\right]. \quad (9)$$

In (9), when $\boldsymbol{j} = \boldsymbol{k}'$, we have that $\mu_{\boldsymbol{k}'}^{(\boldsymbol{k})}$ is the conditional expectation of (5) given $\boldsymbol{k}$ and satisfies

$$\mu_{\boldsymbol{k}'}^{(\boldsymbol{k})} = E\left[\alpha_{\boldsymbol{k}} + \sum_{\boldsymbol{j}\neq\boldsymbol{k},\boldsymbol{k}'} V_{\boldsymbol{j}}^{(\boldsymbol{k})} \middle| \boldsymbol{k}\right] = \alpha_{\boldsymbol{k}} + \sum_{\boldsymbol{j}\neq\boldsymbol{k},\boldsymbol{k}'} \mu_{\boldsymbol{j}}^{(\boldsymbol{k})}$$

and $(\sigma_{\boldsymbol{k}'}^{(\boldsymbol{k})})^2$ is the conditional variance of (5) given $\boldsymbol{k}$, satisfying

$$\left(\sigma_{\boldsymbol{k}'}^{(\boldsymbol{k})}\right)^2 = \mathrm{Var}\left(\sigma_{\boldsymbol{k}'}^{(\boldsymbol{k})}|\boldsymbol{k}\right) = \sum_{\boldsymbol{j}\neq\boldsymbol{k},\boldsymbol{k}'} \left(\sigma_{\boldsymbol{j}}^{(\boldsymbol{k})}\right)^2.$$

Observe that when $\boldsymbol{j} \neq \boldsymbol{k}'$, in (9) we have

$$\frac{\mu_{\boldsymbol{j}}^{(\boldsymbol{k})}}{\sigma_{\boldsymbol{j}}^{(\boldsymbol{k})}} = \frac{\sigma_i \ln\left[P(\boldsymbol{s_j})/P(\boldsymbol{s_k})\right]}{\sqrt{(s_{i1}-s_{i0})^2}} + \frac{s_{i0}^2 - s_{i1}^2}{2\sigma_i\sqrt{(s_{i1}-s_{i0})^2}} + \frac{s_{i1}-s_{i0}}{\sigma_i\sqrt{(s_{i1}-s_{i0})^2}} s_{i0} \quad (10)$$

where i is determined by (7). Now, letting

$$A_i = \frac{s_{i0}^2 + s_{i1}^2 - 2\gamma_i\sqrt{s_{i0}^2 s_{i1}^2}}{\sigma_i^2} \quad (11)$$

for $i = 1, 2$, (10) can be written as

$$\frac{\mu_{\boldsymbol{j}}^{(\boldsymbol{k})}}{\sigma_{\boldsymbol{j}}^{(\boldsymbol{k})}} = \frac{\ln\left[P(\boldsymbol{s_j})/P(\boldsymbol{s_k})\right]}{\sqrt{A_i}} - \frac{\sqrt{A_i}}{2} \quad (12)$$

where i is determined, again, by (7). Further, when $\boldsymbol{j} = \boldsymbol{k}'$ in (9) we have that

$$\frac{\mu_{\boldsymbol{k}'}^{(\boldsymbol{k})}}{\sigma_{\boldsymbol{k}'}^{(\boldsymbol{k})}} = \frac{\alpha_{\boldsymbol{k}} + \sum_{\boldsymbol{j}\neq\boldsymbol{k}\boldsymbol{k}'} \ln\left[P(\boldsymbol{s_j})/P(\boldsymbol{s_k})\right]}{\sqrt{A_1 + A_2}} - \frac{\sqrt{A_1+A_2}}{2}. \quad (13)$$

Hence, each term of the inner sum of (9) can be written in terms of A_1 and A_2. More specifically, (9) is decreasing in both A_1 and A_2. Thus, to minimize (9) we must maximize A_1 and A_2. Hence, to determine the optimal energy allocations E_{10} and E_{20}, we can maximize A_1 and A_2 under the average energy constraint given by (1).

We also notice that (11) is analogous to [2, Eq. (7)] and, with the appropriate modifications, to [3, Eq. (1)]. Thus, to minimize (9) one can use the methods from [2], [3] to show that the optimal energy allocation of Transmitter i is given by

$$E_{i0} = \frac{E_i}{2p_i}\left[1 + \frac{1-2p_i}{\sqrt{1-4p_i(1-p_i)\left(1-\gamma_i^2\right)}}\right] \quad (14)$$

$$E_{i1} = \frac{E_i}{2(1-p_i)}\left[1 - \frac{1-2p_i}{\sqrt{1-4p_i(1-p_i)\left(1-\gamma_i^2\right)}}\right] \quad (15)$$

when $\gamma_i \in [-1, 0)$ and

$$E_{i0} = E_i/p_i \text{ and } E_{i1} = 0 \quad (16)$$

when $\gamma_i \in [0, 1]$.

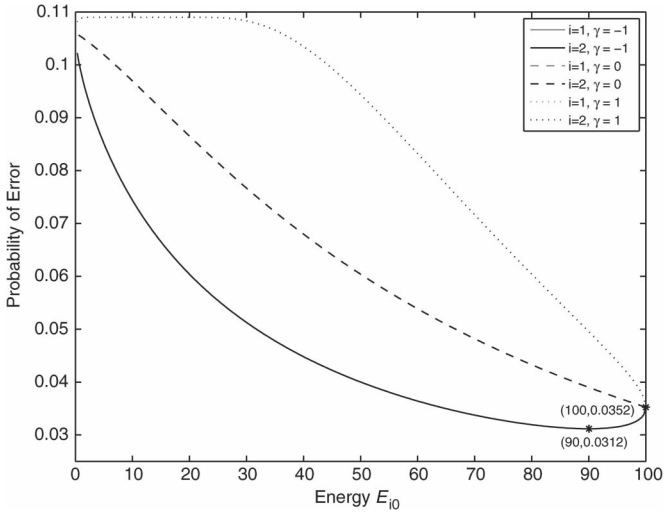

Fig. 1. Numerical analysis under the average energy constrain of $E_1 = E_2 = 10$. Here, $p_1 = p_2 = 0.1$, $\rho = 0.9$, and $\sigma_1 = \sigma_2 = 4$. Note that in this plot the grey and black lines overlap exactly.

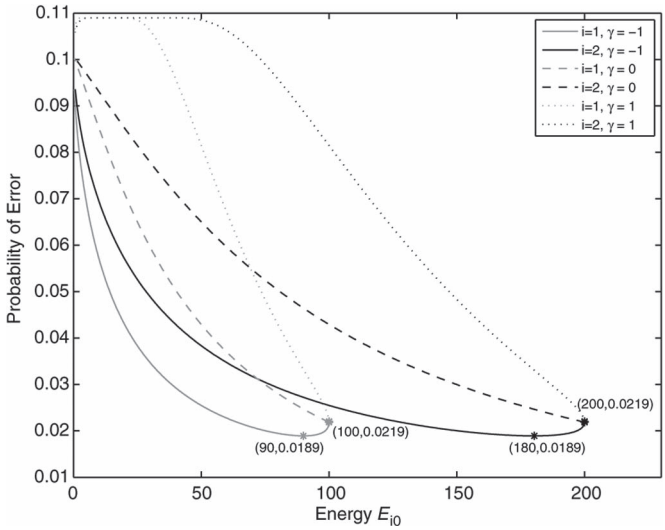

Fig. 2. Numerical analysis under the average energy constrain of $2E_1 = E_2 = 10$. Here, $p_1 = p_2 = 0.1$, $\rho = 0.9$, and $\sigma_1 = \sigma_2 = 4$.

C. Comparison of the Union Bound and the Error Probability

There appears to be no simple way for analytically optimizing the probability of symbol error $P(e)$ given in (8). We can however show numerically that the values which minimize the union bound $P_{UB}(e)$ in (9), also minimize (8).

In Figs. 1 and 2, we use $E_1 = E_2 = 10$ and $2E_1 = E_2 = 20$, respectively. Also, $p_1 = p_2 = 0.1$, $\rho = 0.9$, and $\sigma_1 = \sigma_2 = 4$ and $\gamma_1 = \gamma_2$. In these plots the "$*$" point shows the location of the numerically determined minimum achieved on the interval $[0, E_i/p_i]$. For these test values we conclude that the optimal energy allocations seen in (14)–(16), which minimize (9), also minimize (8). It should be noted that the numerical optimization was also performed for many other values of the system parameters including when $\gamma_1 \neq \gamma_2$. In all cases, we obtained that the optimal energy allocation determined by minimizing the union bound also minimizes the probability of error.

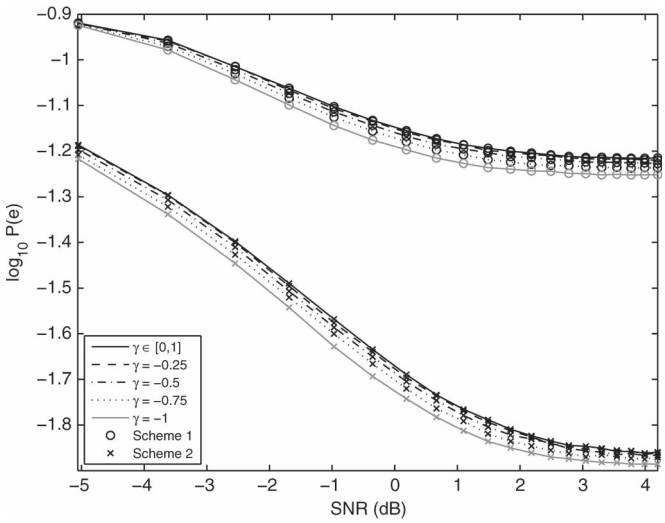

Fig. 3. Performance comparison of Schemes 1 and 2 when $E_1 = 2$.

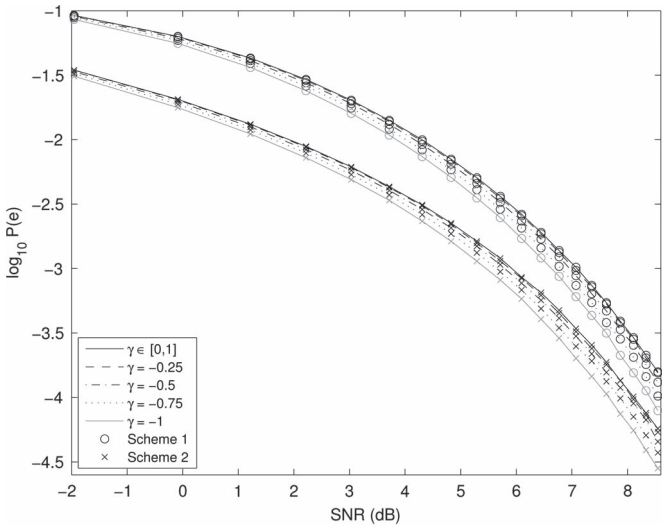

Fig. 4. Performance comparison of Schemes 1 and 2 when $2E_1 = E_2$.

IV. Performance Analysis

We have shown that the optimal energy allocations for binary non-uniform signaling over a single-user system and over the OMAGC coincide. In this section, we assess the benefits, via simulation, of the OMAGC system over independent single-user systems. For the simulations we denote by Scheme 1 and Scheme 2 the two independent single-user systems and the OMAGC system, respectively. Note that both schemes implement the optimal energy allocations; thus, the difference between the two schemes is that the decoder of Scheme 2 exploits the dependence in the source components. In particular, with the true underlying source correlation set at $\rho = 0.9$, Schemes 1 and 2 use a knowledge of ρ for their decoders given by $\hat{\rho}_1 = 0$ and $\hat{\rho}_2 = 0.9$, respectively (i.e., Scheme 1 uses two independent MAP detectors, while Scheme 2 employs joint MAP detection). The following parameters are used in the simulation: $p_1 = p_2 = 0.9$, and $\sigma_1 = \sigma_2 = 2$. In Fig. 3 we use $E_1 = 2$ and in Fig. 4 we use $2E_1 = E_2$. We choose to show the results for $2E_1 = E_2$ since it has similar performance to $E_1 = E_2$ (not shown here). The value E_1 is held constant in Fig. 3 since as the signal-to-noise ratio (SNR), defined by $(E_1 + E_2)/(\sigma_1^2 + \sigma_2^2)$, increases, the difference in average energy between the two transmitters also increases, and thus this setting gives a boundary case at high SNRs. Note that choosing a value for E_1 that is larger than 2 provides similar performance trends with an error floor forming at higher SNRs than in the case of $E_1 = 2$. In summary, when $E_2 = 2E_1$, as seen in Fig. 4, Scheme 2 realizes over Scheme 1 a gain ranging from 0.67 to 0.8 dB (depending on the value of γ) at high SNRs. Similar gains are achievable when $E_1 = E_2$. However, when $E_2 \gg E_1$, as seen in Fig. 3, the performance improvement is quite large, with a minimal gain of 5.8 dB for $\gamma = -1$ and $P(e) \approx 10^{-1.2}$; the gains are much larger for smaller $P(e)$ target values.

V. Conclusion

Based on the analysis of the probability of joint symbol error and the corresponding union error bound derived for the OMAGC channel, we have shown that the optimal energy allocations coincide with the single-user case from [2], [3]. This result can be intuitively inferred by noting that as the two transmitters have no capacity to communicate with each other, the non-interfering (orthogonal) nature of the channel makes the optimal energy allocation dependent only on the marginal distribution of the source. Also, through simulation we have shown that the use of joint detection as implemented in the OMAGC is everywhere better that two independent single-user systems. In particular, when $E_2 = 2E_1$ or $E_1 = E_2$, we have a performance gain of up to 0.8 dB at high SNRs. When $E_2 \gg E_1$, the performance gain is drastically increased with a smallest realizable gain of 5.8 dB. Future work will include similar analysis to that seen in this letter on the traditional multiple access Gaussian channel where the two users interfere with each other.

References

[1] M. Liu, N. Patwari, and A. Terzis, Eds., "Special issue on sensor network applications," *Proc. IEEE*, vol. 98, no. 11, Nov. 2010, pp. 1804–1807.
[2] I. Korn, J. P. Fonseka, and S. Xing, "Optimal binary communication with nonequal probabilities," *IEEE Trans. Commun.*, vol. 51, no. 9, pp. 1435–1438, Sep. 2003.
[3] V. P. Ipatov, "Comments on "Optimal binary communications with nonequal probabilities"," *IEEE Trans. Commun.*, vol. 55, no. 1, p. 231, Jan. 2007.
[4] F. Alajaji, N. Phamdo, and T. Fuja,"Channel codes that exploit the residual redundancy in CELP-encoded speech," *IEEE Trans. Speech Audio Process.*, vol. 4, no. 5, pp. 325–336, Sep. 1996.
[5] G. Takahara, F. Alajaji, N. C. Beaulieu, and H. Kuai, "Constellation mappings for two-dimensional signaling of nonuniform sources," *IEEE Trans. Commun,*, vol. 51, no. 3, pp. 400–408, Mar. 2003.
[6] H. Nguyen and T. Nechiporenko, "Quaternary signal sets for digital communications with nonuniform sources," in *Proc. IEEE CCECE/CCGEI*, May 2005, pp 2085–2088.
[7] B. Moore, G. Takahara, and F. Alajaji, "Pairwise optimization of modulation constellations for non-uniform sources," *IEEE Can. J. Elect. Comput. Eng.*, vol. 34, no. 4, pp. 167–177, Fall 2009.
[8] L. Wei and I. Korn, "Optimal M-ASK/QASK with non-equal symbol probabilities," *IET Commun.*, vol. 5, no. 6, pp. 745–752, Apr. 2011.
[9] L. Wei, "Optimized M-ary orthogonal and bi-orthogonal signaling using coherent receiver with non-equal symbol probabilities," *IEEE Commun. Lett.*, vol. 16, no. 6, pp. 793–796, Jun. 2012.
[10] H. Kuai, F. Alajaji, and G. Takahara, "Tight error bounds for nonuniform signaling over AWGN channels," *IEEE Trans. Inf. Theory*, vol. 46, no. 7, pp. 2712–2718, Nov. 2000.
[11] H. H. Nguyen and N. H. Tran, "Bonferroni-type bounds for CDMA systems with nonuniform signalling," *IEEE Commun. Lett.*, vol. 9, no. 7, pp. 583–585, Jul. 2005.
[12] L. Szczeciński, S. Aissa, C. Gonzalez, and M. Bacic, "Exact evaluation of bit- and symbol-error rates for arbitrary 2-D modulation and nonuniform signaling in AWGN channel," *IEEE Trans. Commun.*, vol. 54, no. 6, pp. 1049–1056, 2006.